The Neural Underpinings of Simultanagnosia: Disconnecting the Visuospatial Attention Network

Magdalena Chechlacz[1,2], Pia Rotshtein[1], Peter C. Hansen[1], Jane M. Riddoch[1,2], Shoumitro Deb[1], and Glyn W. Humphreys[1,2]

Abstract

■ Because of our limited processing capacity, different elements of the visual scene compete for the allocation of processing resources. One of the most striking deficits in visual selection is simultanagnosia, a rare neuropsychological condition characterized by impaired spatial awareness of more than one object at time. To decompose the neuroanatomical substrates of the syndrome and to gain insights into the structural and functional organization of visuospatial attention, we performed a systematic evaluation of lesion patterns in a group of simultanagnosic patients compared with patients with either (i) unilateral visuospatial deficits (neglect and/or extinction) or (ii) bilateral posterior lesions without visuospatial deficits, using overlap/subtraction analyses, estimation of lesion volume, and a lesion laterality index. We next used voxel-based morphometry to assess the link between different visuospatial deficits and gray matter and white matter (WM) damage. Lesion overlap/subtraction analyses, lesion laterality index, and voxel-based morphometry measures converged to indicate that bilateral parieto-occipital WM disconnections are both distinctive and necessary to create symptoms associated with simultanagnosia. We also found that bilateral gray matter damage within the middle frontal area (BA 46), cuneus, calacarine, and parieto-occipital fissure as well as right hemisphere parietal lesions within intraparietal and postcentral gyri were associated with simultanagnosia. Further analysis of the WM based on tractography revealed associations with bilateral damage to major pathways within the visuospatial attention network, including the superior longitudinal fasciculus, the inferior fronto-occipital fasciculus, and the inferior longitudinal fasciculus. We conclude that damage to the parieto-occipital regions and the intraparietal sulcus, together, with bilateral WM disconnections within the visuosptial attention network, contribute to poor visual processing of multiple objects and the loss of processing speed characteristic of simultanagnosia. ■

INTRODUCTION

Visual attention provides us with the ability to select and process a subset of behaviorally relevant visual stimuli while ignoring the rest of visual scene. Within a visual display, many different elements strive for neural representation and the allocation of processing resources. The process of forming neural representations for these elements is competitive because of our limited processing capacity and the need to ensure that behaviorally relevant information gets priority. Functional models of visual attention stress the competition for selection and the modulating role of both bottom–up salience and behavioral prioritization in this process (Bundesen, 1990; Duncan & Humphreys, 1989). Data on the neural underpinnings of the selection system come from both single-unit recordings and functional neuroimaging studies, which converge to highlight the critical role of a fronto-parietal network in mediating the selection of specific visual locations. Evidence on the necessary role of these regions comes also from lesion symptom mapping studies of patients with various visual and spatial attention deficits (e.g., Chechlacz et al., 2010; Verdon, Schwartz, Lovblad, Hauert, & Vuilleumier, 2010; Medina et al., 2009; Karnath, Fruhmann Berger, Kuker, & Rorden, 2004; Mort et al., 2003). One particularly interesting disorder is simultanagnosia, a rare neuropsychological condition characterized by impaired spatial awareness of more than one object at time (Rizzo & Vecera, 2002; Bálint, 1909).

Simultanagnosia provides a unique opportunity to study the nature of human visuospatial processing as it reflects a (largely) nonlateralized deficit in selecting multiple objects (Dalrymple, Birmingham, Bischof, Barton, & Kingstone, 2011; Riddoch et al., 2010; Rizzo & Vecera, 2002; Robertson, Treisman, Friedman-Hill, & Grabowecky, 1997). Wolpert (1924) described simultanagnosia as an inability to interpret a complex visual scene (processing multiple items and the relations between them), despite preservation of the ability to apprehend individual items. Simultanagnosia has also been associated with deficits in global processing (Shalev, Mevorach, & Humphreys, 2007; Shalev, Humphreys,

[1]University of Birmingham, [2]Oxford University

& Mevorach, 2005; Jackson, Swainson, Mort, Husain, & Jackson, 2004; Karnath, Ferber, Rorden, & Driver, 2000), although studies have also demonstrated that global processing may take place implicitly (Shalev et al., 2005; Jackson et al., 2004; Karnath et al., 2000; see also Demeyere, Rzeskiewicz, Humphreys, & Humphreys, 2008). In detailed attempts to assess simultanagnosia in relation to formal accounts of attention, for example, using the Theory of Visual Attention (Bundesen, 1990), Duncan et al. (1999, 2003) argued that a deficit in the rate of visual processing might be critical, over and above the problems in visual STM or biases in spatial selection. This slowing of information processing could reflect impaired subcortical pathways over and above the damage to cortical regions. Therefore, understanding the extent and detailed location of subcortical disconnections in simultanagnosia may provide key insights into not only the neuropathology of simultanagnosia but also the necessary role of structural connections within the visuospatial attention network.

Simultanagnosia leading to poor scene interpretation has been reported primarily in patients with bilateral parietal (e.g., Clavagnier, Fruhmann Berger, Klockgether, Moskau, & Karnath, 2006) and occipital lesions (Rizzo & Hurtig, 1987; see Rizzo & Vecera, 2002, for a review). There have also been some documented cases following either left or right unilateral parietal brain damage (Clavagnier et al., 2006; Naccache, Slachevsky, Levy, & Dubois, 2000; Karpov, Meerson, & Tonkonogii, 1979) but at least in some of these unilateral cases (Clavagnier et al., 2006; Naccache et al., 2000) the lesions have included damage to the corpus callosum, consistent with impaired interhemispheric transfer of visual information. Notably, current understanding of simultanagnosia has been limited largely to case studies, making it difficult to fully assess and decompose the underlying neuronal substrates.

Simultanagnosia can also co-occur with visual neglect and extinction, noted from Bálint's (1909) original case onward, but previous work fails to specify the neuroanatomical relationship between simultanagnosia and other associated visuospatial disorders (see Rizzo & Vecera, 2002). The areas of damage in these syndromes seem to overlap, both within the cortex (e.g., damage within the angular gyrus has been reported in both neglect and simultanagnosia; Chechlacz et al., 2010; Hillis et al., 2005; Mort et al., 2003; Rizzo & Vecera, 2002) and subcortically (Riddoch et al., 2010; Bartolomeo, Thiebaut de Schotten, & Doricchi, 2007). Understanding common and distinct patterns of lesions in patients with different visuospatial deficits could potentially contribute to understanding organization and functional specialization within the visuospatial attention network.

To provide a neuroanatomical analysis of simultanagnosia, we first performed a systematic evaluation of lesion patterns in a group of patients suffering from the disorder. The lesion distribution in this group of patients was next compared with patterns of lesions in two groups of "control" patients with (i) either left or right unilateral visuospatial attention deficits (neglect and/or extinction) and (ii) bilateral posterior lesions but without any visuospatial deficits. In addition, lesion patterns in simultanagnosia patients were compared with lesions in a sample of consecutive patients admitted to the Behavioural Brain Sciences Centre at Birmingham University with the presence of a variety of neuropsychological symptoms and who were not preselected based on any anatomical criteria. The integrity of gray matter (GM) and white matter (WM) was evaluated using advanced MRI sequences: high-resolution T1, T2 FLAIR, and diffusion tensor imaging (DTI). To provide converging evidence for the structure–function relationships, we analyzed the data using lesion overlap and subtraction methods and also employed whole-brain statistical analyses (voxel-based morphometry [VBM]; Ashburner & Friston, 2000) to assess the link between visuospatial deficits and GM and WM damage. To test the hypothesis that bilateral disconnections contribute to the symptoms of simultanagnosia, we computed a laterality index based on lesion volume and lesion location. Finally, to test the hypothesis that simultanagnosia symptoms are associated with neuroanatomical disconnection, we used a streamline tractography approach to specifically evaluate the integrity of WM pathways that are known to be associated with visual processing and spatial awareness connecting the occipital, parietal, and frontal cortices: superior longitudinal fasciculus (SLF), inferior longitudinal fasciculus (ILF), and inferior fronto-occipital fasciculus (IFOF). The current study differs from earlier reports in terms of sample size and data analysis methods. Previous studies were typically based on a single case report; by contrast, we based our findings on a group of seven patients, which provides the basis for more detailed anatomical analyses. Simultanagnosia remains a rare condition, and although a group of seven patients represents a substantially large sample size for such condition, the size of the sample itself presents some limitations. Therefore, as described above, this study aimed to employ and contrast different neuroimaging methods to draw converging conclusions about anatomical substrates of simultanagnosia and not to reflect a particular data analysis method.

The results are discussed in relations to the anatomical dissociations between simultanagnosia and unilateral visuospatial attention deficits, as well as the functional organization of the interconnected networks underlying visuospatial attention. We conclude that our lesion symptom mapping findings advance our understanding of the functional underpinnings of simultanagnosia, which at a functional level are consistent with Duncan et al.'s (2003) argument linking simultanagnosia to severe impairments in visual processing speed.

METHODS

Participants

Patients

Fifty-nine patients participated (43 men and 16 women), with ages ranging from 20 to 85 years (mean age = 61.1 years),

and were divided into experimental and control groups. All patients had acquired brain lesions (stroke, vasculitis, and degenerative changes), were at a chronic stage (>9 months postinjury), and had no contraindications to MRI scanning. No other exclusion criteria were used. All the patients were recruited from the panel of neuropsychological volunteers established in the Behavioural Brain Sciences Centre at the School of Psychology, University of Birmingham. All patients provided written informed consent in agreement with ethics protocols at the School of Psychology and Birmingham University Imaging Centre.

The experimental group consisted seven patients with simultanagnosia (SM). All of these patients also had either neglect or visual extinction, with their problem in visuospatial processing tending to be worse on one side (typically the left). For the purpose of lesion subtraction analyses, three different matched control groups were used: (i) patients with a unilateral lesion and contralateral visuospatial deficits, either neglect and/or extinction (seven with left- and seven with right-side deficits; groups LVS [left visuospatial deficits] and RVS [right visuospatial deficits], respectively), and (ii) seven patients with bilateral parietal and/or occipital lesions but without visuospatial deficits (Bilat group; these patients were selected based on presence of bilateral posterior lesions within either parietal or occipital cortices). For the VBM analyses, an unbiased sample of 52 chronic neurological patients who did not show any of simulatanagnosia symptoms served as the control group. Note that this group included 27 patients with some degree of visuospatial deficit (15 with left- and 12 with right-side deficits). See Tables 1 and 2 for full clinical and demographic data.

Healthy Controls

For the lesion identification protocol (see below), we acquired T1-weighted images from 100 healthy controls (55 men and 45 women, mean age = 54.5 years, range = 20–87 years) with no history of stroke, brain damage, or neurological disorders. We also acquired control data set from 20 healthy control participants (13 men and 7 women, mean age = 60.5 years) for DTI tractography. All controls provided written informed consent in agreement with ethics protocols at the School of Psychology and Birmingham University Imaging Centre.

Behavioral Measures

Simultanagnosia Assessment

Simultanagnosia was diagnosed as a clinical deficit in reporting the gist of a scene shown for at least 2 sec, which is more than sufficient for control participants to realize the scene's gist (see below; if necessary patients were given unlimited time until it was clear that the patient was unable to report the gist and that any problem was not because of naming difficulties, slow or slurred speech, etc.). There were eight black and white line drawings of scenes from everyday life, and the scenes were chosen so that the gist could be gained from the information on either the left or right of the scenes; thus, the problems in understanding the gist should not be because of lateralized deficits. The diagnosis was based on the evaluation whether patients were able to interpret the overall meaning of the scene/gist or only reported isolated single items. In addition simultanagnosia was diagnosed as a clinical deficit based on the duration required to achieve a successful report of two letters (each 0.5°) presented using E-Prime software (Psychology Software Tools), each centered 2° from fixation (1° above and 1° below to minimize unilateral spatial deficits; see Kinsbourne & Warrington, 1962). Performance on this task was also assessed in 10 age-matched controls. None of the controls had difficulty in describing the gist of the scenes at the presentation durations used, and all

Table 1. Patients' Details: Clinical and Demographic Data (All 59 Patients)

	*Simultanagnosia (SM) (n = 7; *n = 5)*	*Controls (n = 52)*
Mean age in years (*SD*)	62.7 ± 7.7 (*61.6 ± 9.2)	61.3 ± 14.5
Sex	3 women, 4 men (*2 women, 3 men)	13 women, 39 men
Etiology	5 stroke, 2 CBD (*4 stroke, 1 CBD)	49 stroke, 1 CBD, 2 HSE
Lesion side	7 bilateral (*5 bilateral)	14 bilateral, 13 left, 25 right
Mean time postlesion in years (*SD*)	6.7 ± 6.7 (*5.0 ± 5.6)	4.9 ± 5.0
Simultanagnosia	7 (*5)	0
Allocentric neglect	5 left (*3 left)	8 left, 1 right
Egocentric neglect	3 left, 2 right (*1 left, 2 right)	6 left, 4 right
Visual extinction	6 left (*4 left)	13 left, 8 right
Visual field defects	1 left	2 left, 3 right

CBD = cortico-basal degeneration; HSE = herpes simplex encephalitis. As we were unable to obtain DTI data for all simultanagnosic patients, the asterisk and numbers in brackets indicate clinical and demographic data for patients who underwent DTI scan.

Table 2. Patient Details: Clinical and Demographic Data (Patients Selected for Lesion Overlap/Subtraction Analyses)

	SM (n = 7)	*LVS Controls (n = 7)*	*RVS Controls (n = 7)*	*Bilateral Controls (n = 7)*
Age in years, mean ± *SD*	62.7 ± 7.7	67.3 ± 8.5	67.3 ± 14.7	65.4 ± 13.7
Sex	3 women	7 men	1 woman	2 women
	4 men		6 men	5 men
Etiology	5 stroke	7 stroke	7 stroke	5 stroke
	2 CBD			2 HSE
Lesion side	7 bilateral	7 right	7 left	7 bilateral
Time postlesion in years, mean ± *SD*	6.7 ± 6.7	4.9 ± 3.5	4.6 ± 3.4	10 ± 7.8
Simultanagnosia	7	0	0	0
Allocentric neglect	5 left	4 left	2 right	0
Egocentric neglect	5 = 3 left, 2 right	4 left	2 right	0
Visual extinction	6 left	4 left	5 right	0
Visual field defects	1 left	1 left	1 right	0

were able to report the two letters shown for 50 msec. Patients were classed as having simultanagnosia if they both made errors on at least three of eight scenes and if they required letter presentations of 200 msec or more to report both letters. Where patients had naming difficulties, semantic circumlocutions that described the nature of the scenes were counted as correct.

Visuospatial Attention Battery

To measure the visuospatial deficits of egocentric neglect, allocentric neglect, and visual extinction, we carried out cognitive assessment with a battery of tests from Birmingham University Cognitive Screen, including Apple Cancellation and Visual Extinction Tests. Full details of the tests are available on-line (www.bucs.bham.ac.uk). The diagnosis of neglect was based on Apple Cancellation task, which is similar to the gap detection task by Ota, Fujii, Suzuki, Fukatsu, and Yamadori (2001), and is designed to simultaneously measure allocentric and egocentric neglect (see Bickerton, Samson, & Humphreys, 2011; Chechlacz et al., 2010). Patients were classed as having a clinical deficit on measures of egocentric and allocentric neglect and visual extinction if their scores on the Apple and Visual Extinction tests fell outside the norms for the tests taken from 86 control participants with no history of neurological diseases (35 men and 51 women, mean age = 67 years, range = 47–88 years). Furthermore, for clear-cut diagnosis of visual extinction, we additionally used a computer task consisting 48 single item and 48 bilateral letter detection trials. For full details, see Supplementary Material. Control norms for visual extinction computer test were assessed based on performance of 10 control participants with no history of neurological diseases and no lesions on MRI scans (5 men and 5 women, age range = 62–74 years). Cutoffs to classify patients as having visual extinction were calculated on the basis of bilateral asymmetry scores (left- vs. right-side errors). Control participants made a maximum of two errors on a single side or both sides, and therefore, the asymmetry scores of >2 were classified as abnormal. Patients were classified as having visual extinction if they fulfilled criteria of at least one of the tests.

Neuroimaging Assessment

Patients and healthy controls were scanned at the Birmingham University Imaging Centre on a 3-T Philips Achieva MRI system with an eight-channel phased array SENSE head coil. Patients' scans were obtained in proximity to the time of behavioral testing. The anatomical scan was acquired using a sagittal T1-weighted sequence (sagittal orientation, echo time (TE)/repetition time (TR) = 3.8/8.4 msec, voxel size = $1 \times 1 \times 1$ mm^3), and for 49 patients, we were able to acquire an additional T2 FLAIR sequence (TR = 11000 msec, TE = 125 msec, voxel size $0.45 \times 0.44 \times 2$ mm^3). We acquired DTI data for 25 healthy controls and five patients with simultanagnosia employing EPI (64 slices with isotropic $2 \times 2 \times 2$ mm^3 voxels, TR = 6170 msec, TE = 78 msec). DTI was acquired in 61 gradient directions with a b value of 1500 sec/mm^2, and 1 volume was acquired with no diffusion weighting (b = 0 image).

Image Preprocessing

T1 scans from patients and healthy controls were first converted and reoriented using MRICro (Chris Rorden, Georgia Tech, Atlanta, GA). Preprocessing was done in SPM5 (Welcome Department of Cognitive Neurology, London, UK). The brain scans were transformed into the

standard Montreal Neurological Institute (MNI) space using the unified segmentation procedure (Ashburner & Friston, 2005). The unified segmentation procedure involves tissue classification based on the signal intensity in each voxel and on a priori knowledge of the expected localization of GM, WM, and CSF in the brain. To further improve tissue classification and spatial normalization of lesioned brains, we used a modified segmentation procedure (Seghier, Ramlackhansingh, Crinion, Leff, & Price, 2008). This protocol was developed to resolve problems with misclassification of damaged tissue by including an additional prior for an atypical tissue class (an added "extra" class) to account for the "abnormal" voxels within lesions and thus allowing classification of the outlier voxels (Seghier et al., 2008). Whereas earlier versions of SPM struggled with normalizing and segmenting brains containing large lesions (e.g., Stamatakis & Tyler, 2005), the unified segment procedure as implemented in SPM5 has been shown to be optimal for spatial normalization of lesioned brains (Crinion et al., 2007). Following segmentation, we visually inspected each of the segmented scans to assess whether segmentation and normalization was successful. Finally, the segmented images were smoothed with a 8-mm FWHM Gaussian filter to accommodate the assumption of random field theory used in the statistical analysis (Worsley, 2003). The choice of intermediate smoothing of 8 mm FWHM was previously shown to be optimal for lesion detection and further analysis of segmented images (e.g., Leff et al., 2009; Seghier et al., 2008; Stamatakis & Tyler, 2005). The preprocessed GM and WM images were used for automated lesion identification using fuzzy clustering (Seghier et al., 2008) and in the voxel-based analyses to determine the relationships between lesion site and simultanagnosia.

Lesion Mapping and Analysis

Automated Lesion Identification

Lesion maps from individual patients were reconstructed using a modified segmentation procedure (see above) and an outlier detection algorithm based on fuzzy clustering (for a description of the full procedure including validation based on real and simulated lesions on T1-weighted scans, see Seghier et al., 2008). This procedure identifies voxels that are different in the lesioned brain as compared with a set of healthy controls (here we employed a set of 100 healthy controls as described above) using normalized GM and WM segments. The GM and WM outlier voxels are then combined into a single outlier image and thresholded to generate a binary map of the lesion (Seghier et al., 2008). The results of lesion reconstruction were verified against each patient's T1 and T2 FLAIR scans. The anatomical localization of the lesion sites for patients with simultanagnosia was based on the Duvernoy Human Brain Atlas (Duvernoy, Cabanis, & Vannson, 1991) and the Woolsey Brain Atlas (Woolsey, Hanaway, & Gado, 2008). The lesion volumes for each patient were calculated using Matlab 7.5 (The MathWorks, Natick, MA) based on binary lesion maps. Subsequently, we applied GM and WM masks defined using the WFU Pick atlas software toolbox in conjunction with SPM5 (Maldjian, Laurienti, Kraft, & Burdette, 2003) to calculate GM and WM lesion volumes for each patient.

Lesion Overlaps and Subtractions

The lesion comparisons across patients were done with SPM5 using Image Calculator functions. To estimate lesion overlap within the experimental groups (SM), a single color set was used with colors ranging from dark to light, coding values representing the number of patients having a lesion to a particular brain area. To estimate differences in lesion location (i.e., to calculate brain regions that were lesioned in one group of patients but spared in other group), subtraction plots were computed. The lesion subtraction plots use two different color sets (one for positive and one for negative values) with colors ranging from dark to light, coding increasing frequencies. Subtraction analyses were computed for the following groups: (1) SM versus LVS, (2) SM versus RVS, and (3) SM versus Bilat. The results were displayed using MRIcron.

VBM

Overlap/subtraction analyses involve calculating the number or proportion of patients with damage within a specific region based on selecting groups (typically matched in size) of patients with or without specific behavioral deficits. These traditional lesion overlap/subtraction methods may be insufficient to precisely identify brain–behavior relationship because of both behavioral (small sample) and anatomical biases. These methods also do not control for the effects of potentially covarying factors, such as age, time since lesion, and lesion volume that could affect cognitive performance. More importantly, these methods do not take into account variability between patients, hence cannot assess the reliability of the observations. Such limitations can be overcome by using more robust statistical analyses carried out without prior patient selection. Therefore, to complement our lesion overlap/subtraction analysis, we next applied a voxel-wise statistical approach to assess the link between the cognitive deficits in simultanagnosia and brain damage using normalized and smoothed GM and WM images.

To assess the relationship between WM and GM damage and simultanagnosia on a voxel-by-voxel basis, we used a VBM approach (Ashburner & Friston, 2000) and carried out statistical analyses with SPM5 using smoothed GM and WM maps obtained from segmented scans from our patient sample (see above for the preprocessing protocol). We used parametric statistics within the framework of the general linear model (Kiebel & Holmes, 2003), and the analyses for WM and GM were carried out separately. In each statistical model age, handedness, gender, type of lesion, time since diagnosis, and lesion volume were

included as covariates of no interest. All these covariates ensured that we could control for various confounding factors that might potentially have affected cognitive performance. The analyses included all 59 patients (see above and Table 1 for details). In our analyses, we asked three questions: (1) What are the neural correlates of simultanagnosia (Analysis 1, comparing 7 SM patients to the unbiased sample of 52 patients)? (2) What is the relationship between the neuronal substrates of simultanagnosia and left visuospatial deficits (Analysis 2)? (3) What is the relationship between the neuronal substrates of simultanagnosia and right visuospatial deficits (Analysis 3)? Analyses 2 and 3 aimed to formally test for common and dissociated neuronal substrates that contribute to simultanagnosia and other common visuospatial deficits such as egocentric neglect, allocentric neglect, and visual extinction. Dissociating simultanagnosia from either left visuospatial deficits or right visuospatial deficits was achieved by using exclusive masking, that is, testing for a change in voxel intensity that correlated with simultanagnosia ($p < .001$, uncorrected) but not with either left or right visuospatial deficits ($p > .05$, uncorrected). Common mechanisms were tested by using an inclusive mask—that is, selecting all voxels common to both simultanagnosia and either left or right visuospatial deficits. We report only results that showed significant effect at $p < .001$ FWE-corrected threshold at the cluster level with amplitude of voxels surviving $p < .001$ uncorrected across the whole brain and an extent threshold of 200 mm^3 (>100 voxels). The brain coordinates are presented in standardized MNI space. The anatomical localization of the lesion sites within the GM was based on the Anatomical Automatic Labeling toolbox (Tzourio-Mazoyer et al., 2002), the Duvernoy Human Brain Atlas (Duvernoy et al., 1991), and the Woolsey Brain Atlas (Woolsey et al., 2008). To localize WM lesions associated with visual extinction in relation to specific WM pathways, we used the JHU WM tractography atlas (Hua et al., 2008) and the MRI Atlas of Human White Matter by Mori (2005). The brain coordinates are presented in the standardized MNI space.

Lesion Volume and Laterality Index

In addition to the VBM analyses, we tested whether simultanagnosia is simply associated with larger lesion volume compared with the control patients (i.e., 14 SM vs. 14 unilateral VS + 7 Bilat). Next, to assess whether the symptoms are predominantly related to WM disconnection, we compared lesion volume of the GM and WM. A mixed design ANOVA was used with patient groups (7 SM vs. 14 unilateral VS + 7 Bilat) as the between-participant factor and lesion volume (GM vs. WM lesion volume) as the within-participant factor. Finally, simultanagnosia symptoms have been reported in patients with predominantly bilateral lesions. To test how crucial bilateral occipito-parietal lesions are to the simultanagnosia syndrome, we computed a lesion laterality index based on the lesion volume in the different lobes. The brain region encompassing each lobe was defined using the WFU Pick atlas software toolbox in conjunction with SPM5 (Maldjian et al., 2003). We then calculated a lesion laterality index (i.e., (left − right)/(left + right)) separately for the GM and WM lesions within the frontal, temporal and parieto-occipital lobes. The reliability of differences between the patient groups: SM versus Bilat was computed using a two-sample *t* test. We used Matlab 7.5 (The MathWorks, Natick, MA) and SPSS16 (SPSS, Chicago, IL) for the statistical analyses.

Image Analyses: DTI Data

Data Processing

All DTI data sets were first converted using dcm2nii (Chris Rorden, Georgia Tech, Atlanta, GA) and then analyzed using FSL (FMRIB, Oxford, U.K.). First, all raw data were corrected for distortions because of eddy currents and any movements using FSL eddy correction module within FSL FDT toolbox (Smith et al., 2004).

DTI Tractography

We detected and quantified the extent and laterality of damage within the SLF, ILF, and IFOF based on tractography and tract-specific measures. For the purpose of this analysis, we used the DTI data available for five patients with simultanagnosia (age range = 47–71 years, mean age = 61.6 ± 9.2 years; two women and three men), and for comparison we included DTI data obtained for 20 healthy controls (age range = 45–74 years, mean age = 60.5 ± 9.2 years; 7 women and 10 men). For comparison, we also included in the analysis data from five patients with left visuospatial deficits and right brain lesions (LVS: age range = 53–76 years, mean age = 64.8 ± 8.6; years, five men), five patients with right visuospatial deficits and left brain lesions (RVS: age range = 54–81 years, mean age = 65.2 ± 10.3 years, one woman and four men), seven chronic neurological patients without any visuospatial deficits with either bilateral ($n = 3$) or left ($n = 2$) or right ($n = 2$) brain lesions (CN [chronic neurological]: age range = 40–72 years, mean age = 54.6 ± 10.7 years, three women and four men). Tract reconstruction was performed using Diffusion Toolkit, followed by tract visualization and tract extraction using Trackvis (both programs developed by Ruopeng Wang, Van J. Wedeen, TrackVis.org, Martinos Center for Biomedical Imaging, Massachusetts General Hospital). For tract reconstruction, we used the Fiber Assignment by Continuous Tracking algorithm (Mori, Crain, Chacko, & van Zijl, 1999), as implemented in Diffusion Toolkit. Tracts were propagated along the direction of the primary eigenvector with tracking stopped when either the flip angle threshold was not met (flip angle value was lower than 0.15) or by the angle threshold exceeding 45°. The fiber tracking was first performed from every voxel in the brain and then followed by tract extraction using ROI filters. For extraction of the SLF, a single ROI approach was used, whereas for the ILF and IFOF, two

ROI approaches were used based on the method proposed by Mori et al. (2002), replicated by other research groups (e.g., Singh, Jeong, Hwang, Sungkarat, & Gruen, 2010; Thomas et al., 2009). All tracts were extracted in native diffusion space by one of the authors (M.C.) using systematic protocols created and followed to ensure extraction consistency between participants (for full protocols, see Supplementary Methods and Supplementary Figure 1). We first compared the results of tract reconstruction for each patient with lesion location on a T1-weighted image. Subsequently, the trajectory of each reconstructed tract (in both patients and controls) was checked to ensure consistency with previous studies and neuroanatomical atlases (Catani & Thiebaut de Schotten, 2008; Catani, Howard, Pajevic, & Jones, 2002; Mori et al., 2002) and the number of streamlines for each tract as well as for the whole brain was calculated for all participants. The number of streamlines for the whole brain was used to estimate the overall extent of WM damage in individual patients compared with controls. The total number of streamlines reflects individual differences in brain size and is often used to normalize the results for each tract of interest; however, because of brain lesions in patients (but not in controls) this approach was not applicable in our study. The reliability of differences in the number of reconstructed streamlines between patients and the healthy controls as well as between various groups of patients was computed using a two-sample *t* test. We used Matlab 7.5 (The MathWorks, Natick, MA).

RESULTS

Behavioral Measures

Seven patients were diagnosed with simultanagnosia symptoms. All seven simultanagnosic patients were also diagnosed with left visual extinction. Two of these seven patients suffered from left allocentric and left egocentric neglect, whereas one had right egocentric and left allocentric neglect. Two patients had left allocentric but not egocentric neglect, whereas one patient had left egocentric but not allocentric neglect (see Table 1). Control patients did not have any simultanagnosia symptoms, but several patients suffered from unilateral visuospatial deficits, including 8 patients with left and one with right allocentric neglect, 6 patients with left and four with right egocentric neglect, and 13 patients with left and eight with right visual extinction (see Table 1).

Neuroimaging Results

Lesion Overlap and Subtraction Analyses

We first performed a systematic evaluation of lesion patterns in a group of simultanagnosic (SM) patients based on lesion overlap. The analysis revealed wide bilateral lesion overlap within WM areas and less extensive overlap within GM. Specifically, we found large overlap in the WM areas with maximal lesion overlap (seven of seven SM patients) within bilateral inferior parietal, parieto-occipital and occipital lobes (suggesting damage to association and commissural pathways such as SLF, posterior corona radiata, posterior thalamic radiation, IFOF, ILF, and corpus callosum; Figure 1A, top). Furthermore, SM patients had bilateral lesions in the GM areas of the frontal, parietal, and occipital cortices, although the actual region of maximal overlap (four of seven SM patients) was restricted to the bilateral cuneus, medial part of parieto-occipital fissure, right and, to the lesser extent, also left middle frontal area (BA 46; i.e., middle frontal and inferior frontal gyri) and right inferior parietal lobule including portions of the angular and postcentral gyri (Figure 1A, top).

Overall, the above findings suggest that simultanagnosia symptoms are associated with bilateral lesions to regions in the vicinity of the posterior parietal-occipital and middle frontal cortices. However, not all patients with bilateral lesions to these regions necessarily exhibit simultanagnosic symptoms or indeed any spatial attention deficits (e.g., Bilat Controls, see Figure 1A, bottom). To test which lesions are critically associated with simultanagnosia, we contrasted lesion patterns in the SM group with the Bilat patient group using lesion subtraction analysis. We also compared the lesion pattern in the SM patients with that in patients with unilateral visuospatial deficits only (neglect and extinction—the LVS and RVS groups, see Figure 1A, middle) to separate the neuronal substrates commonly associated with neglect and extinction from those areas specifically associated with simultanagnosia. The subtraction plots showed that bilateral damage in the WM within posterior parietal, parieto-occipital, and occipital lobes were associated with simultanagnosia, but these regions were spared in the control groups (Figure 1B). Moreover, the subtraction plots also demonstrated that bilateral damage in the GM within the cuneus, parieto-occipital fissure, precuneus, and right parietal cortex (including portions of the postcentral and intraparietal gyri) were associated with simultanagnosia, but these regions were spared in all control groups (Figure 1B) Although we also found overlap across some areas of damage within both GM and WM in patients with simultanagnosia, extinction, and neglect (in particular within inferior parietal lobule including the angular gyrus), the subtraction plots clearly show that at least some of the anatomical substrates of simultanagnosia (SM) are separate from those characterizing the other syndromes and, crucially, are bilateral.

Next, we tested whether simultanagnosia is associated with wider spread lesions. We first compared overall lesion volume between the SM patients and those belonging to the three control groups (Bilat + LVS + RVS). On average, lesion volume for the simultanagnosia patients was 47.39 ± 20.35 mm^3 (average ± *SD*) and lesion volume in the control patients was 39.96 ± 34.58 mm^3 (Bilat = 49.27 ± 36.22 mm^3, LVS = 45.29 ± 41.90 mm^3, RVS = 25.32 ± 23.12 mm^3). Overall lesion volume in the simultanagnosia group was not significantly larger than in the other neuropsychological patients ($t(26) = 0.54$, $p > .5$).

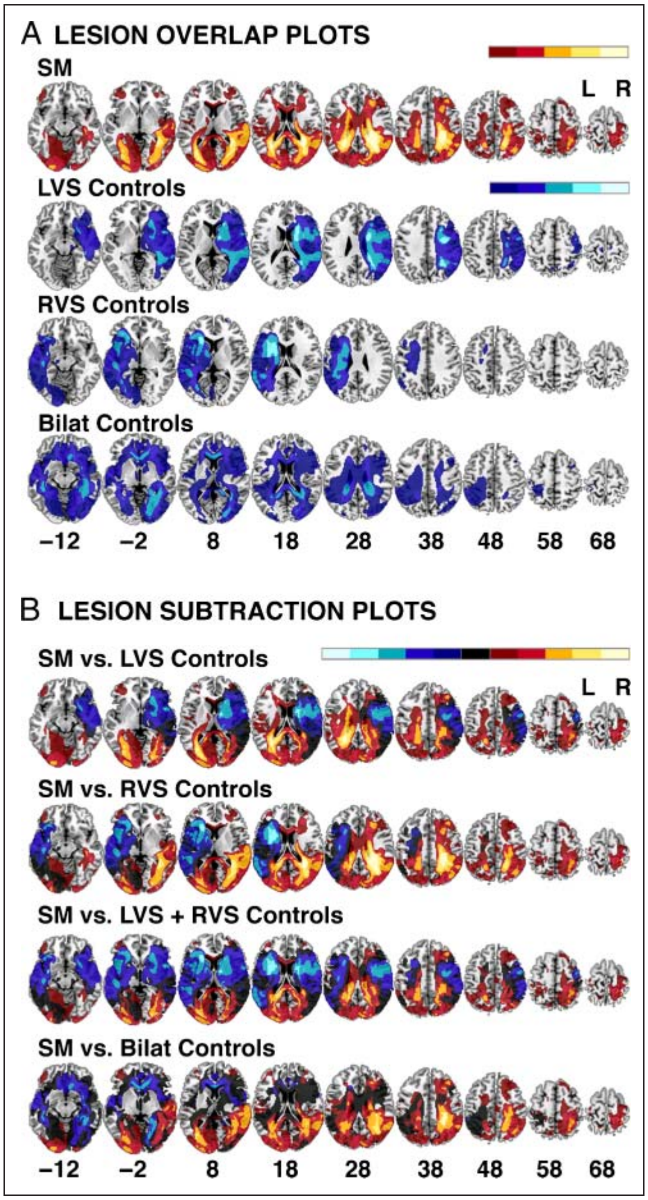

Figure 1. (A) Lesion overlap plots for simultanagnosic patients (SM, $n = 7$) and three control groups without any simultanagnosia symptoms: patients with left visuospatial deficits and right brain lesions (LVS controls, $n = 7$), patients with right visuospatial deficits and left brain lesions (RVS controls, $n = 7$), and patients with bilateral fronto-parieto-occipital lesions but with neither neglect nor extinction (Bilat controls, $n = 7$). The color range indicates the number of patients with overlapping lesions from brown ($n = 1$) to light yellow ($n = 7$) for the simultanagnosic group (SM) and from dark blue ($n = 1$) to pale blue ($n = 7$) for all control groups. (B) Lesion subtraction plots for SM patients versus different control groups as listed above. On subtraction plots warm colors (brown to light yellow) represent brain regions damaged more frequently in patients with simultanagnosia relative to different control groups represented by cold colors (dark blue to pale blue). Note that black (middle of the color bar) indicates regions where the frequency of damage is identical in both groups. The lesion overlap and subtraction plots are presented as an overlay on a standard T1 multislice template in MRIcron (Chris Rorden, Georgia Tech, Atlanta, GA). MNI z coordinates of the axial sections are given. All images are displayed in neurological convention, that is, left of the slice represents the left hemisphere.

This indicates that extent of lesion alone cannot account for simultanagnosia.

The subtraction and overlap analyses suggest that simultanagnosia might be critically linked to WM rather than GM damage. Therefore, we tested whether simultanagnosia might be associated with relatively larger damage to WM than GM. We computed a mixed ANOVA with the following factors: lesion volume (GM, WM) and group (SM, neurological controls, i.e., Bilat + LVS + RVS). We found a significant interaction of lesion volume (GM vs. WM) and patient group (with vs. without simultanagnosia; $F(1, 26) = 4.21$, $p < .05$). This interaction indicated that the volume of WM lesions were significantly larger, compared with GM lesions, in the simultanagnosia patients ($t(6) = -2.90, p < .05$) but not across the neurological control groups ($t(20) = -1.82, p > .08$). Interestingly, the total volume of WM lesions was not significantly larger in the simultanagnosia group (vs. the control patients, $t(26) = 1.26$, $p > .2$). Taken together, these results strongly indicate that simultanagnosia might be chiefly explained by WM disconnection.

Lesion Laterality

To investigate the role of bilateral lesions in simultanagnosia, we computed a lesion laterality index, wherein the closer it is to zero, the higher the bilateral symmetry is. Not surprisingly, the LVS and RVS groups showed clear asymmetrical GM and WM lesions denoted by high laterality scores for all three brain regions (Figure 2A–C), and therefore, they were not included in the follow-up statistical analysis. In contrast, the simultanagnosia patients (SM) showed a low laterality index mostly in parieto-occipital regions within WM (Figure 2C). Supporting this observation, a comparison between the SM patients and the Bilat group showed a significant lower laterality index for parieto-occipital WM lesions in the SM patients ($t(12) = -2.46$, $p < .05$). No other reliable differences were found in the laterality pattern in any other brain regions. The laterality index analyses show that bilateral parieto-occipital WM disconnections are both distinctive and necessary to create simultanagnosia.

VBM

One caveat to the above analyses is that the patients' groups were preselected. This could introduce behavioral and anatomical biases and confounds by failing to rule out cases in the overall neuropsychological population where the damage may be found but the patients are symptomless. To overcome this as well as to control for the effects of potentially covarying factors, such as age, time since lesion, and lesion volume that could potentially affect cognitive performance, we supplemented the above analyses with a VBM approach applied in the context of a large unbiased sample of neuropsychological patients (see results in Tables 3 and 4 and Figures 3 and 4). VBM analyses of

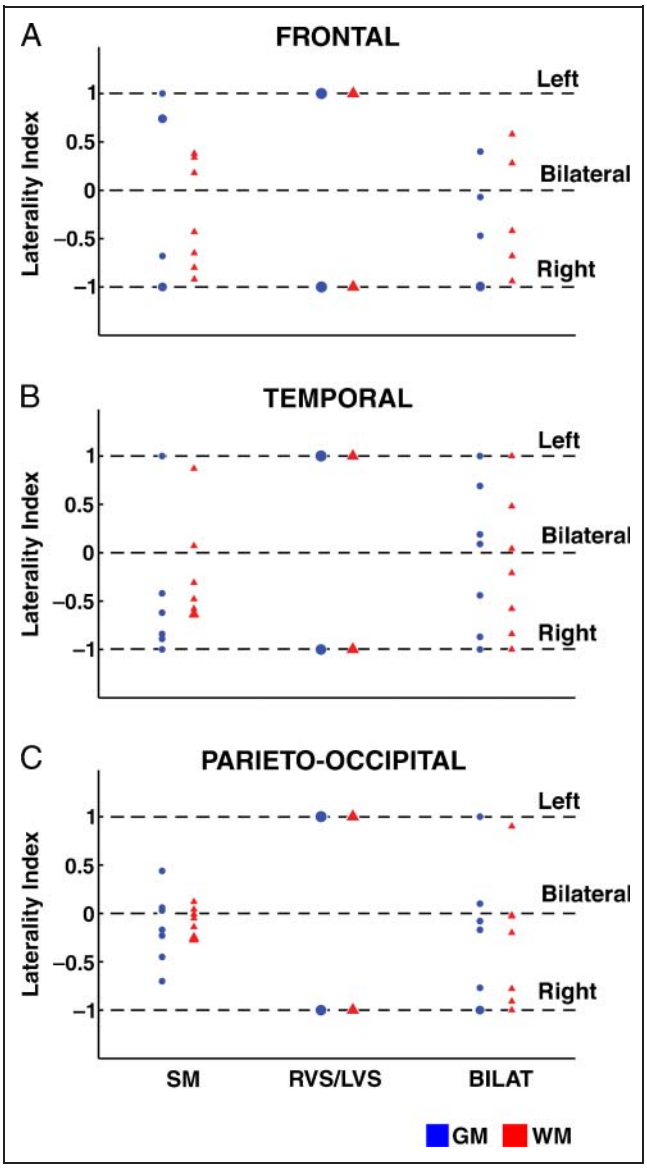

Figure 2. Lesion laterality indices within frontal (A), temporal (B), and parieto-occipital (C) lobes estimated separately for the GM and WM, plotted for patients in the simultanagnosic (SM) group and in three control groups (LVS, RVS, and BILAT; see Methods for details). Blue circles indicate GM, and red triangles indicate WM.

GM damage associated with simultanagnosia indicated lesions within frontal, parietal, and occipital cortices. Specifically, we found a link between simultanagnosia symptoms and GM damage within bilateral calcarine, cuneus and parieto-occipital fissure, left middle and superior occipital gyrus, bilateral middle frontal area (BA 46, i.e., middle frontal and inferior frontal gyri), and superior frontal gyrus, as well as right parietal areas including intraparietal sulcus, postcentral and superior parietal gyri, and angular gyrus (Figure 3A; Table 3, Analysis 1). VBM analysis of the WM damage associated with simultanagnosia indicated bilateral occipital and parieto-occipital lesions (suggesting damage within long association and commissural pathways including, bilaterally, SLF, IFOF, and ILF, corpus callosum, ILF, left corona corona radiata, and left posterior thalamic radiation; Figure 4A; Table 4, Analysis 1).

Similarly to the lesion subtraction plots, in VBM analyses we used statistical models including additional covariate for left or right visuospatial deficits to dissociate simultanagnosia (SM) from unilateral symptoms such as neglect and visual extinction (LVS and RVS deficits). After controlling for unilateral deficits, we found that GM lesions within bilateral calcarine, cuneus and parieto-occipital fissure, left middle and superior occipital gyrus, bilateral middle frontal area (BA 46), bilateral superior frontal gyrus, and right intraparietal sulcus were exclusively associated with simultanagnosia (Figure 3B, C; Table 3, Analysis 2 and Analysis 3). These results also showed that, overall, simultanagnosia symptoms were not associated with damage to the inferior parietal lobule, including the angular gyrus (i.e., areas typically associated with neglect; see Chechlacz et al., 2010; Medina et al., 2009; Hillis et al., 2005; Mort et al., 2003). Interestingly, we found that, whereas bilateral lesions within long association pathways including the SLF, IFOF, and ILF result in simultanagnosia symptoms, unilateral disconnections within these pathways produce contralateral visuospatial deficits (Figure 4A, B; Table 4, Analysis 2 and Analysis 3). Similar results (albeit with weaker reliability) were obtained when we tested for the correlation between brain damage and simultanagnosia symptoms with the analyses based only on data from stroke patients (not shown).

DTI Tractography

To further characterize the WM lesions, we next used data and analyses procedures optimized for WM based on DTI. Information solely derived from the conventional T1-weighted MRIs is not sufficient to accurately depict damage within specific WM tracts. Therefore, to further examine WM substrates of simultanagnosia, we examined the extent and laterality (left and right hemisphere changes in structural connectivity) of damage within a priori tracts of interests: SLF, IFOF, and IFOF. We used streamline tractography and tract-specific measures to directly evaluate damage within the three major tracts of interests: SLF, ILF and IFOF. Tract reconstruction was computed for the five simultanagnosic patients and 20 age-matched healthy controls as well as for five LVS patients, five RVS patients, and seven chronic neurological patients without any visuospatial deficits. The results are presented in Figure 5. Within the healthy controls, we observed large variability in the number of reconstructed streamlines for each fasciculus. This variability is expected when taking into account age differences across the control group (see, e.g., Thomas et al., 2008). We nevertheless did not weight or correct the healthy control results by age or gender as this group was chosen to match the simultanagnosic patients, and we wanted to avoid the need to apply any data transformations to the patients' data. Note that variability in the control data reduces the likelihood of finding reliable

Table 3. GM Substrates of Simultanagnosia

	Cluster Level		*Voxel Level*	*Coordinates*			
Contrast	p_{FWE}	*Size*	*z Score*	*x*	*y*	*z*	*Brain Structure (Location)*
Simultanagnosia							
VBM: Analysis 1	.000	1687	5.79	−28	−94	4	Left MOG and SOG, calcarine, cuneus, parieto-occipital fissure
	.000	2085	5.36	−28	34	40	Left MFG and IFG, bilateral SFG
			5.32	−8	66	8	
			5.12	8	64	0	
	.000	551	5.26	36	34	36	Right IFG and MFG
	.000	1049	4.89	28	−34	62	Right postcentral and superior parietal gyri, intraparietal sulcus and angular gyrus
			4.87	24	−60	56	
	.000	400	4.72	10	−82	28	Right calcarine, parieto-occipital fissure, cuneus
Simultanagnosia Excluding LVS Deficits							
VBM: Analysis 2	.000	435	6.10	−28	36	42	Left MFG and IFG
	.000	1137	5.58	−30	58	8	Left MFG and SFG
	.000	1332	5.37	−30	−92	4	Left MOG and SOG, calcarine, cuneus, parieto-occipital fissure
	.000	598	5.19	−6	66	6	Bilateral SFG
			4.90	8	64	0	
	.000	505	4.75	34	30	44	Right IFG and MFG
	.000	255	4.25	26	−92	22	Right calcarine, parieto-occipital fissure, cuneus
	.000	121	3.94	30	−68	58	Right intraparietal sulcus
Simultanagnosia Excluding RVS Deficits							
VBM: Analysis 3	.000	1468	5.77	−30	−92	4	Left MOG and SOG, calcarine, cuneus, parieto-occipital fissure
	.000	1840	5.35	−28	34	40	Left MFG and IFG, bilateral SFG
			5.18	−8	66	4	
			5.13	8	64	0	
	.000	371	5.22	36	34	36	Right IFG and MFG
	.000	1018	4.80	28	−34	62	Right postcentral and superior parietal gyri, intraparietal sulcus and angular gyrus
			4.79	24	−60	56	
	.000	403	4.73	10	−82	28	Right calcarine, parieto-occipital fissure, cuneus

IFG = inferior frontal gyrus; MFG = middle frontal gyrus; MOG = middle occipital gyrus; SFG = superior frontal gyrus; SOG = superior occipital gyrus.

differences between the controls and the individual simultanagnosic patients.

We found that overall, the number of reconstructed streamlines across both hemispheres was significantly lower in simultanagnosic patients compared with healthy controls ($t(23) = -3.84$, $p < .001$), which converges with the extensive WM damage in the SM group, as demonstrated above by lesion analyses (Figure 5A). Tractography confirmed lesion overlap and VBM findings suggesting that lesions associated with simultanagnosia indeed affect bilaterally structural integrity of three long association pathways: SLF, IFOF, and ILF (Figure 5B–D). We found a significant reduction in the number of streamlines in simultanagnosia patients compared with healthy controls within left ($t(23) = -4.10$, $p < .0005$) and right ($t(23) = -8.28$, $p < .0001$) SLF, left ($t(23) = -3.0$, $p < .01$) and right ($t(23) = -4.35$,

Table 4. WM Substrates of Simultanagnosia

	Cluster Level		*Voxel Level*	*Coordinates*			
Contrast	p_{FEW}	*Size*	*z Score*	*x*	*y*	*z*	*Brain Structure (Location)*
Simultanagnosia							
VBM: Analysis 1	.000	1783	4.16	−28	−84	6	Left IFOF, ILF, post. TR
			4.04	−26	−56	34	Left SLF, post. CR, IFOF, corpus callosum, post. TR
	.000	243	3.83	28	−42	34	Right SLF, IFOF, ILF
Simultanagnosia Excluding LVS Deficits							
VBM: Analysis 2	.000	2109	4.35	−28	−82	6	Left IFOF, ILF, post. TR
			4.27	−18	−100	14	Left IFOF, post. CR
			4.13	−26	−56	36	Left SLF, post. CR, IFOF, corpus callosum, post. TR
Simultanagnosia Excluding RVS Deficits							
VBM: Analysis 3	.000	167	4.02	28	−42	34	Right SLF, IFOF, ILF

CR = corona radiata; post. = posterior; TR = thalamic radiation.

$p < .0005$) IFOF, as well as left ($t(23) = -5.23, p < .0001$) and right ($t(23) = -3.51, p < .005$) ILF.

We next performed tracts reconstruction for three additional patients group: with left visuospatial deficits (LVS), right visuospatial deficits (RVS), and chronic neurological patients without any visuospatial deficits (CN). We used two-sample *t* test to compare the results of each patient group to the healthy controls. We note that, because of the small number of patients in each group, these results should be considered with cautious. The number of reconstructed streamlines for the CN group did not differ from that of the healthy controls (both across the whole brain and for individual WM tracts). Not surprisingly, we found a significant reduction in the number of reconstructed streamlines in LVS patients compared with healthy controls within right SLF ($t(23) = -5.57, p < .0001$) and right IFOF ($t(23) = -3.75, p < .001$). We also found a significant reduction in the number

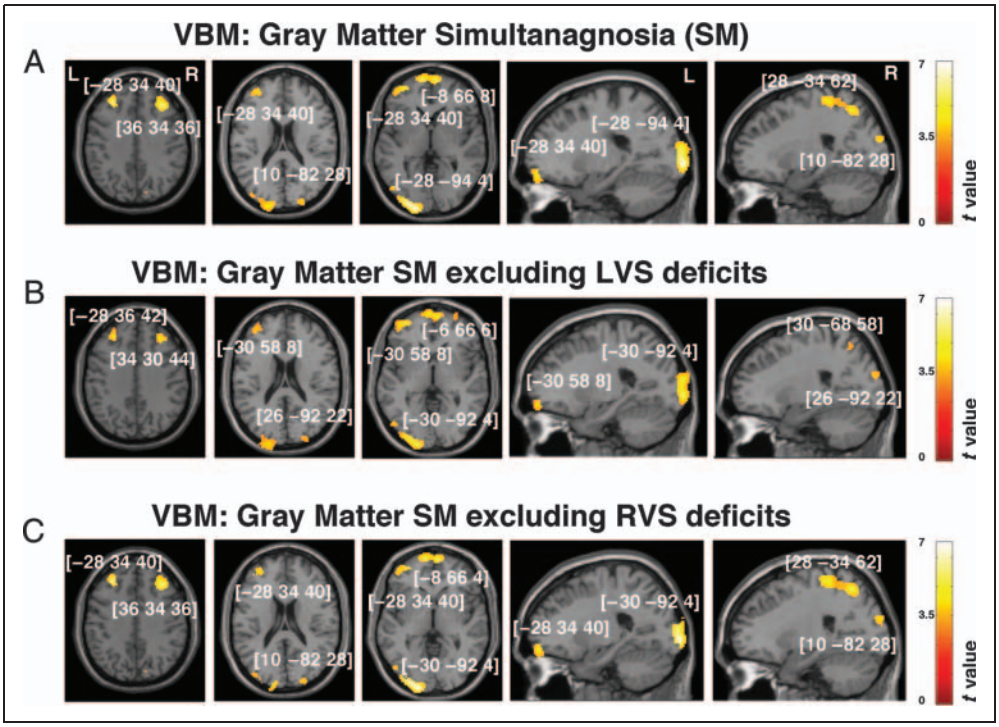

Figure 3. (A) GM substrates of simultanagnosia (SM)—results from the VBM analysis designed to test the relationship between reduced GM volume (GM lesions) and simultanagnosia symptoms (Analysis 1). GM substrates of simultanagnosia versus unilateral left (B) and right (C) visuospatial deficits. Dissociating simultanagnosia from either left visuospatial deficits (Analysis 2) or right visuospatial deficits (Analysis 3) was achieved by using exclusive masking. See Methods for details of statistical models. SPMs are overlaid on canonical T1 image. All images are displayed in neurological convention, that is, the left of the slice represents the left hemisphere. Numbers in brackets indicate peak MNI coordinates.

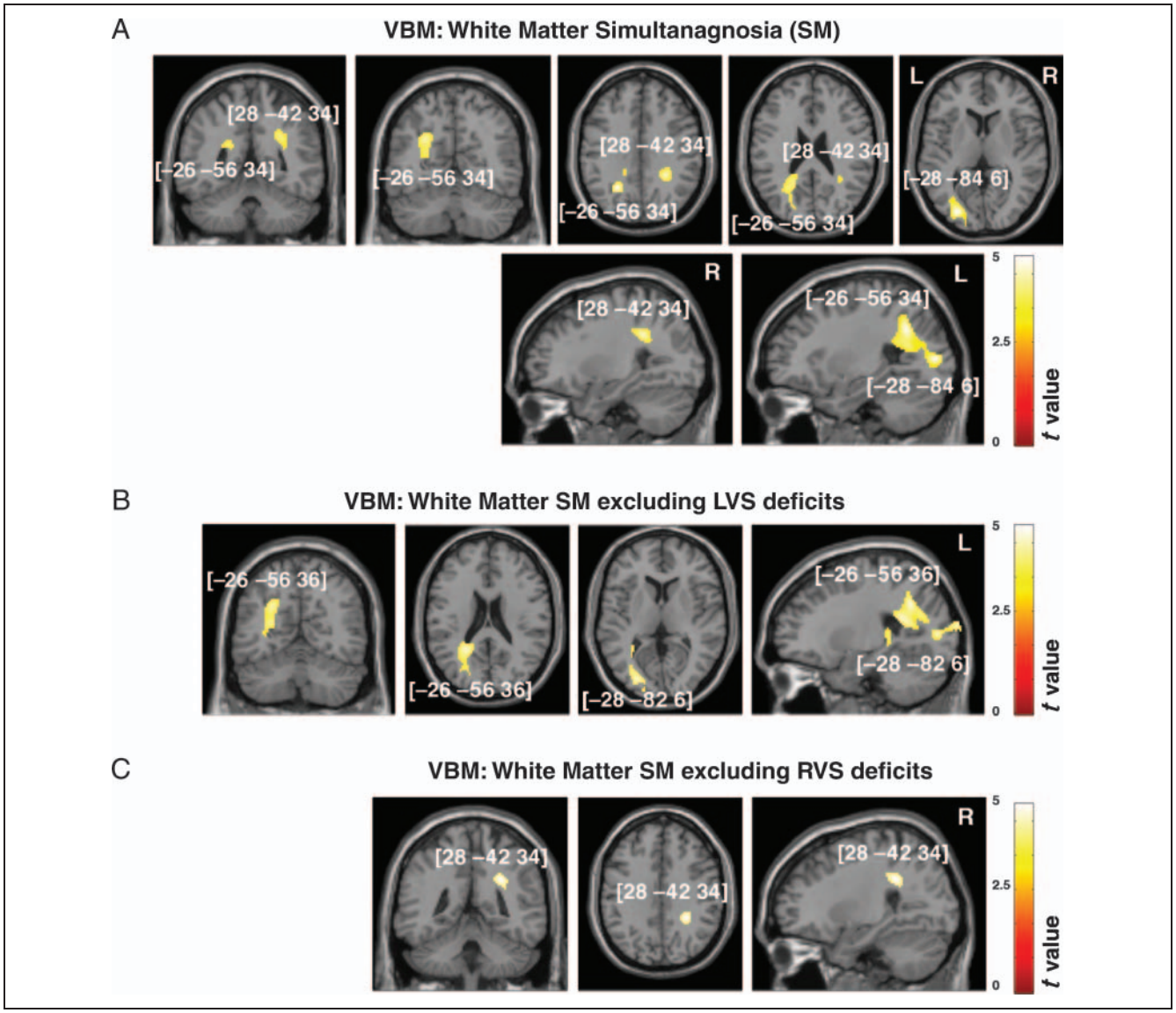

Figure 4. (A) WM substrates of simultanagnosia (SM)—results from the VBM analysis designed to test the relationship between reduced WM volume (WM lesions) and simultanagnosia symptoms (Analysis 1). WM substrates of simultanagnosia versus unilateral left (B) and right (C) visuospatial deficits. Dissociating simultanagnosia from either left visuospatial deficits (Analysis 2) or right visuospatial deficits (Analysis 3) was achieved by using exclusive masking. See Methods for details of statistical models. SPMs are overlaid on canonical T1 image. All images are displayed in neurological convention, that is, the left of the slice represents the left hemisphere. Numbers in brackets indicate peak MNI coordinates.

of reconstructed streamlines in RVS patients compared with healthy controls within left IFOF ($t(23) = -3.59, p < .005$). These results are consistent with previous reports indicating unilateral damage within these WM pathways in patients with contralateral visuospatial deficits (e.g., Chechlacz et al., 2010; Thiebaut de Schotten et al., 2008; Urbanski et al., 2008). There was no significant difference in the number of reconstructed streamlines within these damaged WM tracts between the simultanagnosia patients and patients with unilateral visuospatial deficits (right SLF: SM vs. LVS, $t(8) = 0.05, p > .5$; right IFOF: SM vs. LVS, $t(8) = -0.47$, $p > .5$; left IFOF: SM vs. RVS, $t(8) = 1.02, p > .1$). Thus, the magnitude of any WM tract disconnection within one hemisphere was not critical for simultanagnosia symptoms, but the presence of bilateral damage to fiber pathways was. Taken together, the tractography analyses revealed that visuospatial attention deficits in simultanagnosic patients were associated with bilateral lesions (significant reduction in structural connectivity) within all three examined long association pathways, the SLF, IFOF, and ILF interconnecting fronto-parieto-occipital regions.

DISCUSSION

To date, the understanding of simultanagnosia has been limited largely to case studies, making it difficult to assess the underlying neuronal substrates. Although bilateral parieto-occipital and posterior parietal (including angular

gyrus) lesions have been reported, these also occur in combination with damage within other brain regions including frontal cortex and pulvinar (Jackson et al., 2004; Rizzo & Vecera, 2002; Humphreys, Cinel, Wolfe, Olson, & Klempen, 2000; Coslett & Saffran, 1991; Ogren, Mateer, & Wyler, 1984; Hausser, Robert, & Giard, 1980; Holmes, 1918; Bálint, 1909). In the current study, we evaluated the contrasting GM and WM substrates of (i) simultanagnosia (SM) versus

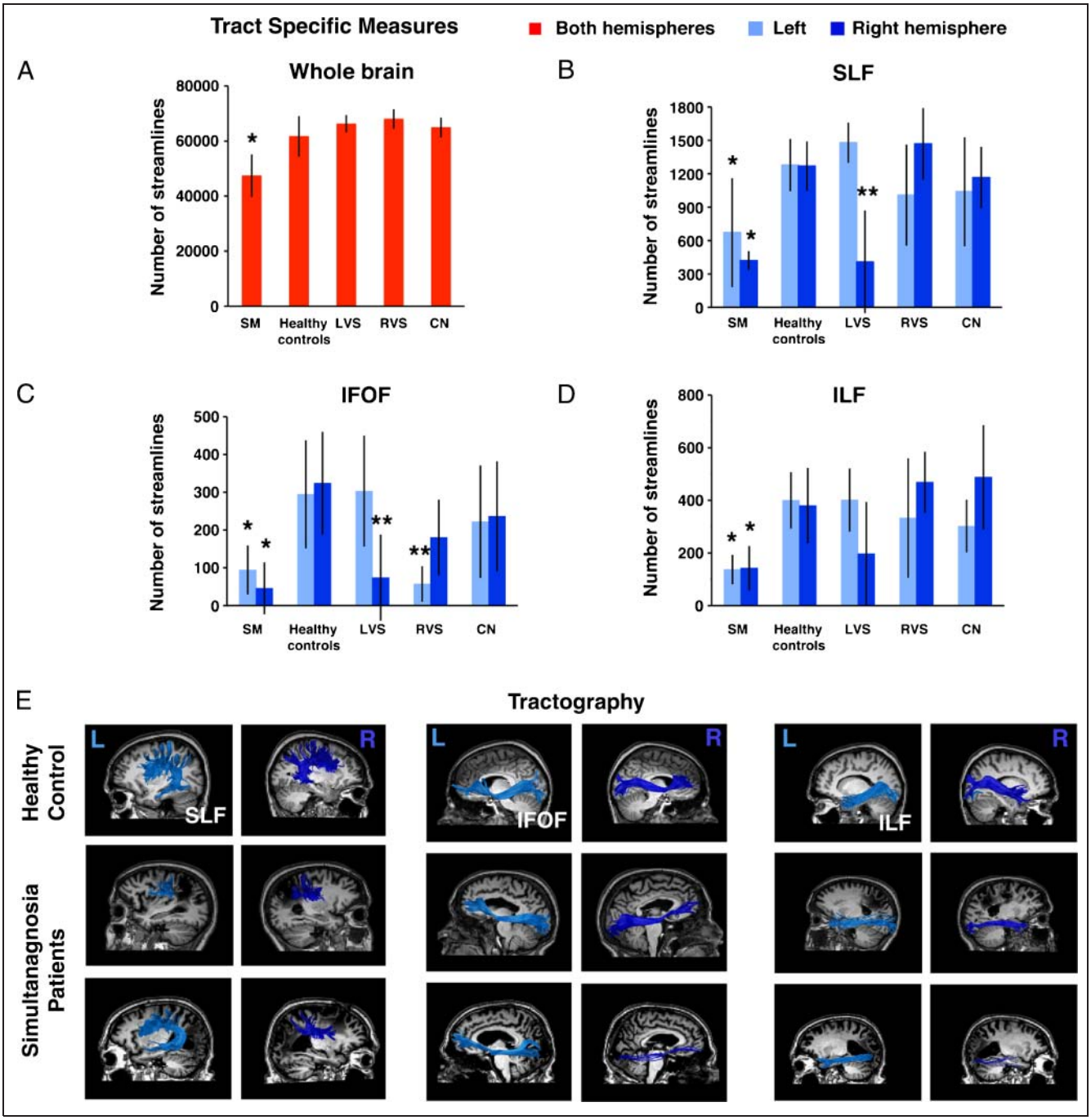

Figure 5. The number of reconstructed streamlines for the whole brain (A) and the three fasciculi (B–D; SLF, IFOF, and ILF; left and right hemisphere separately) in simultanagnosic (SM) patients (n = 5), patients with left visuospatial deficits and right brain lesions (LVS, n = 5), patients with right visuospatial deficits and left brain lesions (RVS, n = 5), chronic neurological patients without any visuospatial deficits with either bilateral or left or right brain lesions (CN, n = 7), and age matched healthy controls (n = 20). In A–D, the error bars indicate standard deviations; * indicates fasciculi with significantly reduced structural integrity in simultanagnosic patients, and ** indicates fasciculi with significantly reduced structural integrity in control patient groups (LVS, RVS, CN), that is, the number of streamlines was significantly reduced compared with controls ($p < .01$; see Results for details). (E) Examples of reconstructed IFOF, ILF, and SLF for one of the healthy controls and two of the simultanagnosic patients. The tracts are displayed on a corresponding T1 scan in parasagittal view. L = left hemisphere (light blue); R = right hemisphere (dark blue); whole brain = both hemispheres (red).

co-occurring visuospatial deficits (neglect/extinction), (ii) simultanagnosia versus bilateral control patients without visuospatial deficits, and (iii) an unbiased sample of neurological patients to decompose the neuroanatomical substrates of the syndrome and to gain insights into structural and functional organization of visuospatial attention networks. The bilateral disconnection account of simultanagnosia was also examined using DTI imaging. Importantly, despite using various lesion symptom mapping approaches, the results converge to provide strong and reliable evidence for the neural substrates of simultanagnosia.

Simultanagnosia as a Disconnection Syndrome

The results indicated that, along with any associated cortical damage, the symptoms associated with simultanagnosia are linked to extensive disconnection within WM pathways subserving visual processing and spatial attention. As noted in the Introduction, simultanagnosic deficits have been attributed to severe impairments in visual processing speed (Duncan et al., 1999, 2003) in accordance with the Theory of Visual Attention (Bundesen, 1990). Our findings fit with this idea in the sense that deficits in processing speed might follow from extensive bilateral WM disconnections. Further analyses revealed that bilateral parieto-occipital WM disconnections within the syndrome are both distinctive (see below for discussion in relation to neglect and organization of visuospatial attention network) and necessary to create symptoms associated with simultanagnosia.

We used tractography to provide direct evidence of disconnection within major parieto-occipital and fronto-occipital networks in simultanagnosia. We examined structural integrity within three long association tracts: the SLF connecting frontal, parietal and temporal cortices, the ILF connecting temporal and occipital cortices, and the IFOF connecting frontal and occipital cortices. We found that simultanagnosia is associated with damage within all three long association pathways. It has been proposed that cognitive deficits in simultanagnosia affect different aspects of spatial attention, including the consolidation of information into visual working memory and thus the link between damage to either left or right ILF and impaired visual recent memory (Tusa & Ungerleider, 1985) might provide one of the keys to understanding at least some simultanagnosia symptoms. Previous studies point to SLF as one of the main components of the fronto-parietal attention network (Petrides & Pandya, 2006; Schmahmann & Pandya, 2006; Makris et al., 2005; Mesulam, 1981) and disruptive connectivity within right SLF has been reported in connection with behavioral deficits in the neglect syndrome (Chechlacz et al., 2010; Karnath, Rorden, & Ticini, 2009; Thiebaut de Schotten et al., 2008; Bartolomeo et al., 2007). The IFOF links the occipital and frontal lobes and passes under parietal cortex. Previous work has suggested that the direct fronto-parietal connection is critical for attention, spatial, and visual processing (Doricchi, Thiebaut de Schotten, Tomaiuolo, & Bartolomeo, 2008; Fox, Iaria, & Barton, 2008; Aralasmak et al., 2006). Additionally, it has been proposed that right or bilateral damage within the IFOF, in conjunction with damage to posterior parietal cortex, could result in impaired simultaneous perception as well as causing optic ataxia and oculomotor apraxia (Aralasmak et al., 2006; Battelli, Cavanagh, Martini, & Barton, 2003; Stasheff & Barton, 2001; Ghika, Ghika-Schmid, & Bogousslasvky, 1998). Interestingly, some of our simultanagnosia patients also suffered from other symptoms of full Balint's syndrome, that is, optic ataxia and oculomotor apraxia (not reported here) and taking into account individual differences in the lesion pattern and severity of symptoms, further work is needed to link the severity of Bálint's symptoms to the extent of loss of structural integrity within IFOF and other long association pathways. Nevertheless, we propose here that bilateral damage to the parieto-occipital cortex and the right intraparietal sulcus, together with underlying bilateral WM lesions, contributes to poor visual processing of multiple objects and the loss of processing speed in simultanagnosia, whereas additional fronto-parieto-occipital disconnections might result in increased severity of symptoms and further visuospatial problems.

Visuospatial Attention Network: Simultanagnosia and Other Neuropsychological Syndromes

The current study provides strong evidence that, although the areas of damage in patients with simultanagnosia, extinction, and neglect can partially overlap, the cortical substrates of simultanagnosia symptoms can be separated from those characterizing the other syndromes. In particular, our data indicate that simultanagnosia is associated with damage to the middle frontal area (BA 46), parieto-occipital and middle occipital regions; in contrast to this, neglect is typically associated with lesions including the temporal parietal junction, superior temporal gyrus and angular gyrus (Chechlacz et al., 2010; Hillis et al., 2005; Karnath et al., 2004; Mort et al., 2003; Vallar, Bottini, & Paulesu, 2003; Vallar, 2001). One reason why we did not find these areas associated with simultanagnosia here is that we extracted[1] out areas related to unilateral impairments. Our data, however, contradict the argument that simultanagnosia/Bálint's syndrome constitutes a form of double neglect, at least in terms of cortical damage (Farah, 1990). However, could there be a form of double neglect generated through subcortical disconnection? Damage within the right SLF, IFOF, and ILF has been reported in neglect patients (ILF: Bird et al., 2006; SLF: Chechlacz et al., 2010; Thiebaut de Schotten et al., 2008; He et al., 2007; IFOF: Chechlacz et al., 2010; Urbanski et al., 2008) and bilateral damage within these tracts is found in simultanagnosia. One account of these data is that the WM damage common to the disorders reflects a slower rate of information processing (cf. Duncan et al., 1999, 2003), and this may exacerbate the spatial biases leading to neglect and extinction (see Robertson & Manly, 1999). This

would be less a form of "double neglect" than an additional contributing factor that is nevertheless functionally distinct from the spatial bias that is key to neglect and extinction. In simultanagnosia, the pronounced WM damage leads to the slowed processing being the dominant factor and to generally poor awareness of multiple stimuli.

Although, the double neglect account of simultanagnosia is not plausible, undoubtedly the current study provides evidence that both simultanagnosia and unilateral visuospatial attention deficits result from disconnection within a common neuronal network (see Figures 4 and 5). Although distinct cortical regions seem to control shifts of attention, visual selection, target detection, and so on, common WM pathways support interactions across these different cortical regions. The organization of neuronal network for visuospatial attention has been examined recently by a study using probabilistic tractography approach to investigate structural connectivity between neuronal substrates of attention identified based on functional imaging (Umarova et al., 2010). The study proposed a visuospatial attention network consisting both dorsal (connecting temporo-parietal with frontal regions) and ventral (traveling from temporo-parietal regions toward the pars triangularis of the inferior frontal gyrus, insula, and putamen) pathways. The dorsal pathways identified by Umarova et al. (2010) have been assigned to the SLF (most likely to two of its subcomponents, SLFII and SLFIII) and the ventral pathway to either anterior IFOF or ILF and the external capsule fiber system. Because of the nature of the paradigm used, the above study (Umarova et al., 2010) only described the components of the visuospatial attention network within the right hemisphere. The results of the current study indicate that a bilaterally organized visuospatial attention network underlies different aspects of visual selection and spatial attention.

Dorsal and Ventral Simultanagnosia

One final point to be raised is the relation between the so-called "dorsal" and "ventral" simultanagnosia, as labeled by Farah (1990). Historically, the term simultanagnosia refers to patients with poor ability to interpret complex visual displays, but in fact it has been often applied in the context of two somewhat different deficits and two different groups of patients (Farah, 1990). Specifically, the term dorsal simultanagnosia has been used to classify poor interpretation of scenes resulting from impaired spatial awareness of more than one object at time and has been mainly linked to bilateral parieto-occipital lesions (Farah, 1990; Luria, 1959; Wolpert, 1924). In contrast, ventral simultanagnosia has been noted after unilateral damage to the left posterior ventral cortex mainly involving temporo-occipital regions (see Kinsbourne & Warrington, 1962) and is characterized by symptoms such as alexia and impaired reporting of multiple letters under brief exposure conditions. On one hand, such patients do not show poor interpretation of scenes per se, but their letter-by-letter reading is accompanied by impairment in describing complex pictures despite ability to see more than one object at time (Humphreys & Price, 1994; Kinsbourne & Warrington, 1962).

In the current study patients were classified as having simultanagnosia based on dual-symptom definition (poor scene interpretation plus multiple letter report). Our neuroimaging analyses indicated an association between bilateral parieto-occipital disconnections and the dual-symptom characterization of simultanagnosia representing a deficit that is neither material specific nor linked to a process such as naming (most of our simultanagnosia had no naming problems). Interestingly, our VBM analysis of GM also indicated a link between the symptoms of simultanagnosia and left occipital lesions (i.e., the lesion pattern characteristic for ventral simultanagnosia). This could be partially attributed to the dual symptom characterization of simultanagnosia, but it could also point to functional similarities between dorsal and ventral simultanagnosia. Although Coslett and Saffran (1991) suggested that dorsal and ventral simultanagnosia result from completely different impairments, Duncan et al.'s (2003) findings indicate a common functional deficit, as they showed that both types of patient suffered from severe impairments in processing speed. We conclude that simultanagnosia does represent a general problem such as slowed visual processing that impacts on all tasks requiring the rapid assimilation of visual information across the field.

Methodological Consideration

Simultanagnosia is often reported in patients with different etiologies, including corticobasal degeneration (CBD) and posterior cortical atrophy (e.g., Mendez, 2000; Mendez & Cherrier, 1998). We opted to base our study on a non-preselected clinical cohort with different clinical etiologies (mainly stroke, but also CBD and encephalitis; see Tables 1 and 2) as two of the simultanagnosic patients (of seven included in the study) suffered from CBD. Furthermore, pooling across different neurological etiologies and using VBM facilitates understanding of brain behavior relationships by generalizing the inferences across different causes of brain lesion. Importantly, VBM is sensitive to tissue changes outside the main lesion, including WM and GM atrophy, and this is important as we studied patients in the chronic stage of the disorder. The atrophy may be a factor contributing to the functional deficit at this stage (see Gottesman et al., 2008, for evidence in relation to unilateral visuospatial deficits). However, our approach has limitations. These are mainly because of the fact that the neuroimaging data (anatomical scans only) used here are susceptible to shortcomings in terms of capturing all brain changes contributing to cognitive deficits (e.g., tissue malperfusion). Thus it is possible that we provided here an underestimation of the contribution the relevant brain areas related to simultanagnosia. Further work is required to test this possibility.

Conclusions

We conclude that our findings provide evidence that lesion associated with simultanagnosia are different than those associated with unilateral spatial attention syndromes such as neglect and extinction. The critical lesions associated with simultanagnosia occupy the parieto-occipital and middle occipital regions as well as the middle frontal area (BA 46), whereas lesions within the temporal parietal junction and inferior parietal lobule (angular gyrus) are associated with unilateral symptoms. Furthermore, not only the different pattern of GM lesions but also the bilaterality of WM disconnections in individual neuropsychological patients determine the degree to which visual processing and spatial attention are disrupted and thus the nature of visuospatial deficits. We note that the analysis approach used here specifically tested for lesions that were associated with simultanagnosia while controlling for other spatial attention deficits. Therefore, this study highlights the differences rather than the commonalities across the various spatial attention deficits.

Acknowledgments

The authors would like to thank Dr. Mohamed L. Seghier from Wellcome Trust Centre for Neuroimaging (Institute of Neurology, University College London) for providing us with his Matlab codes for modified unified segmentation and an outlier detection algorithm. This work was supported by grants from the Coventry and Warwickshire Partnership National Health Service Trust (M. C. and S. D.), Leverhulme Trust (P. R.), the MRC and the Stroke Association (G. W. H.).

Reprint requests should be sent to Magdalena Chechlacz, Behavioural Brain Sciences Centre, School of Psychology, University of Birmingham, Birmingham B15 2TT, United Kingdom, or via e-mail: m.chechlacz.1@bham.ac.uk.

Note

1. The primary aim of the presented work was to highlight the differences rather than the commonalities across the various spatial attention deficits. However, please note that we have observed that damage within TPJ was associated with simultanagnosia in some of the examined simultanagnosic patients (not maximum lesion overlap and thus not reported in Results) when compared with patients with nonspatial attention deficits (Bilateral group/Bilat controls; see Figure 1B).

REFERENCES

Aralasmak, A., Ulmer, J. L., Kocak, M., Salvan, C. V., Hillis, A. E., & Yousem, D. M. (2006). Association, commissural, and projection pathways and their functional deficit reported in literature. *Journal of Computer Assisted Tomography, 30,* 695–715.

Ashburner, J., & Friston, K. J. (2000). Voxel-based morphometry—The methods. *Neuroimage, 11,* 805–821.

Ashburner, J., & Friston, K. J. (2005). Unified segmentation. *Neuroimage, 26,* 839–851.

Bálint, R. (1909). Seelenlähmung des "Schauens," optische Ataxie, räumliche Störung der Aufmerksamkeit. *Monatschrift für Psychiatrie und Neurologie, 25,* 51–81.

Bartolomeo, P., Thiebaut de Schotten, M., & Doricchi, F. (2007). Left unilateral neglect as a disconnection syndrome. *Cerebral Cortex, 17,* 2479–2490.

Battelli, L., Cavanagh, P., Martini, P., & Barton, J. J. (2003). Bilateral deficits of transient visual attention in right parietal patients. *Brain, 126,* 2164–2174.

Bickerton, W. L., Samson, D., & Humphreys, G. W. (2011). Separating forms of neglect using the Apples Test: Validation and functional prediction in chronic and acute stroke. *Neuropsychology, 25,* 567–580.

Bird, C. M., Malhotra, P., Parton, A., Coulthard, E., Rushworth, M. F., & Husain, M. (2006). Visual neglect after right posterior cerebral artery infarction. *Journal of Neurology, Neurosurgery, and Psychiatry, 77,* 1008–1012.

Bundesen, C. (1990). A theory of visual attention. *Psychological Review, 97,* 523–547.

Catani, M., Howard, R. J., Pajevic, S., & Jones, D. K. (2002). Virtual in vivo interactive dissection of white matter fasciculi in the human brain. *Neuroimage, 17,* 77–94.

Catani, M., & Thiebaut de Schotten, M. (2008). A diffusion tensor imaging tractography atlas for virtual in vivo dissections. *Cortex, 44,* 1105–1132.

Chechlacz, M., Rotshtein, P., Bickerton, W.-L., Hansen, P. C., Deb, S., & Humphreys, G. W. (2010). Separating neural correlates of allocentric and egocentric neglect: Distinct cortical sites and common white matter disconnections. *Cognitive Neuropsychology, 27,* 277–303.

Clavagnier, S., Fruhmann Berger, M., Klockgether, T., Moskau, S., & Karnath, H. O. (2006). Restricted ocular exploration does not seem to explain simultanagnosia. *Neuropsychologia, 44,* 2330–2336.

Coslett, H. B., & Saffran, E. (1991). Simultanagnosia. To see but not two see. *Brain, 114,* 1523–1545.

Crinion, J., Ashburner, J., Leff, A., Brett, M., Price, C., & Friston, K. (2007). Spatial normalization of lesioned brains: Performance evaluation and impact on fMRI analyses. *Neuroimage, 37,* 866–875.

Dalrymple, K. A., Birmingham, E., Bischof, W. F., Barton, J. J. S., & Kingstone, A. (2011). Experiencing simultanagnosia through windowed viewing of complex social scenes. *Brain Research, 1367,* 265–277.

Demeyere, N., Rzeskiewicz, A., Humphreys, K. A., & Humphreys, G. W. (2008). Automatic statistical processing of visual properties in simultanagnosia. *Neuropsychologia, 46,* 2861–2864.

Doricchi, F., Thiebaut de Schotten, M., Tomaiuolo, F., & Bartolomeo, P. (2008). White matter (dis)connections and gray matter (dys)functions in visual neglect: Gaining insights into the brain networks of spatial awareness. *Cortex, 44,* 983–995.

Duncan, J., Bundesen, C., Olson, A., Humphreys, G., Chavda, S., & Shibuya, H. (1999). Systematic analysis of deficits in visual attention. *Journal of Experimental Psychology: General, 128,* 450–478.

Duncan, J., Bundesen, C., Olson, A., Humphreys, G., Ward, R., Kyllingsbaek, S., et al. (2003). Attentional functions in dorsal and ventral simultanagnosia. *Cognitive Neuropsychology, 20,* 675–701.

Duncan, J., & Humphreys, G. W. (1989). Visual search and stimulus similarity. *Psychological Review, 96,* 433–458.

Duvernoy, H. M., Cabanis, E. A., & Vannson, J. L. (1991). *The human brain: Surface, three-dimensional sectional anatomy and MRI*. Wien: Springer-Verlag.

Farah, M. J. (1990). *Visual agnosia: Disorders of object recognition and what they tell us about normal vision*. Cambridge, MA: MIT Press.

Fox, C. J., Iaria, G., & Barton, J. J. (2008). Disconnection in prosopagnosia and face processing. *Cortex, 44,* 996–1009.

Ghika, J., Ghika-Schmid, F., & Bogousslasvky, J. (1998). Parietal motor syndrome: A clinical description in 32 patients in the acute phase of pure parietal strokes studied prospectively. *Clinical Neurology and Neurosurgery, 100,* 271–282.
Gottesman, R. F., Kleinman, J. T., Davis, C., Heidler-Gary, J., Newhart, M., Kannan, V., et al. (2008). Unilateral neglect is more severe and common in older patients with right hemispheric stroke. *Neurology, 71,* 1439–1444.
Hausser, C. O., Robert, F., & Giard, N. (1980). Balint's syndrome. *Canadian Journal of Neurological Sciences, 7,* 157–161.
He, B. J., Snyder, A. Z., Vincent, J. L., Epstein, A., Shulman, G. L., & Corbetta, M. (2007). Breakdown of functional connectivity in frontoparietal networks underlies behavioral deficits in spatial neglect. *Neuron, 53,* 905–918.
Hillis, A. E., Newhart, M., Heidler, J., Barker, P. B., Herskovits, E. H., & Degaonkar, M. (2005). Anatomy of spatial attention: Insights from perfusion imaging and hemispatial neglect in acute stroke. *Journal of Neuroscience, 25,* 3161–3167.
Holmes, G. (1918). Disturbances of visual orientation. *British Journal of Ophthalmology, 2,* 449–468, 506–516.
Hua, K., Zhang, J. Y., Wakana, S., Jiang, H. Y., Li, X., Reich, D. S., et al. (2008). Tract probability maps in stereotaxic spaces: Analyses of white matter anatomy and tract-specific quantification. *Neuroimage, 39,* 336–347.
Humphreys, G. W., Cinel, C., Wolfe, J., Olson, A., & Klempen, N. (2000). Fractionating the binding process: Neuropsychological evidence distinguishing binding of form from binding of surface features. *Vision Research, 40,* 1569–1596.
Humphreys, G. W., & Price, C. J. (1994). Visual feature discrimination in simultanagnosia—A study of 2 cases. *Cognitive Neuropsychology, 11,* 393–434.
Jackson, G. M., Swainson, R., Mort, D., Husain, M., & Jackson, S. R. (2004). Implicit processing of global information in Balint's syndrome. *Cortex, 40,* 179–180.
Karnath, H. O., Ferber, S., Rorden, C., & Driver, J. (2000). The fate of global information in dorsal simultanagnosia. *Neurocase, 6,* 295–305.
Karnath, H. O., Fruhmann Berger, M., Kuker, W., & Rorden, C. (2004). The anatomy of spatial neglect based on voxelwise statistical analysis: A study of 140 patients. *Cerebral Cortex, 14,* 1164–1172.
Karnath, H. O., Rorden, C., & Ticini, L. F. (2009). Damage to white matter fiber tracts in acute spatial neglect. *Cerebral Cortex, 19,* 2331–2337.
Karpov, B. A., Meerson, Y. A., & Tonkonogii, I. M. (1979). On some peculiarities of the visuomotor system in visual agnosia. *Neuropsychologia, 17,* 281–294.
Kiebel, S., & Holmes, A. (2003). The general linear model. In R. S. J. Frackowiak et al. (Eds.), *Human brain function* (2nd ed., pp. 725–760). San Diego, CA: Academic Press.
Kinsbourne, M., & Warrington, E. K. (1962). A disorder of simultaneous form perception. *Brain, 85,* 461–486.
Leff, A. P., Schofield, T. M., Crinion, J. T., Seghier, M. L., Grogan, A., Green, D. W., et al. (2009). The left superior temporal gyrus is a shared substrate for auditory short-term memory and speech comprehension: Evidence from 210 patients with stroke. *Brain, 132,* 3401–3410.
Luria, A. R. (1959). Disorders of simultaneous perception in a case of bilateral occipito-parietal brain injury. *Brain, 82,* 437–449.
Makris, N., Kennedy, D. N., McInerney, S., Sorensen, A. G., Wang, R., Caviness, V. S., Jr., et al. (2005). Segmentation of subcomponents within the superior longitudinal fascicle in humans: A quantitative, in vivo, DT-MRI study. *Cerebral Cortex, 15,* 854–869.
Maldjian, J. A., Laurienti, P. J., Kraft, R. A., & Burdette, J. H. (2003). An automated method for neuroanatomic and cytoarchitectonic atlas-based interrogation of fMRI data sets. *Neuroimage, 19,* 1233–1239.
Medina, J., Kannan, V., Pawlak, M. A., Kleinman, J. T., Newhart, M., Davis, C., et al. (2009). Neural substrates of visuospatial processing in distinct reference frames: Evidence from unilateral spatial neglect. *Journal of Cognitive Neuroscience, 21,* 2073–2084.
Mendez, M. F. (2000). Corticobasal ganglionic degeneration with Balint's syndrome. *Journal of Neuropsychiatry and Clinical Neurosciences, 12,* 273–275.
Mendez, M. F., & Cherrier, M. M. (1998). The evolution of alexia and simultanagnosia in posterior cortical atrophy. *Neuropsychiatry Neuropsychology and Behavioral Neurology, 11,* 76–82.
Mesulam, M. M. (1981). A cortical network for directed attention and unilateral neglect. *Annals of Neurology, 10,* 309–325.
Mori, S. (2005). *MRI atlas of human white matter*. Amsterdam: Elsevier.
Mori, S., Crain, B. J., Chacko, V. P., & van Zijl, P. C. M. (1999). Three-dimensional tracking of axonal projections in the brain by magnetic resonance imaging. *Annals of Neurology, 45,* 265–269.
Mori, S., Kaufmann, W. E., Davatzikos, C., Stieltjes, B., Amodei, L., Fredericksen, K., et al. (2002). Imaging cortical association tracts in the human brain using diffusion-tensor-based axonal tracking. *Magnetic Resonance in Medicine, 47,* 215–223.
Mort, D. J., Malhotra, P., Mannan, S. K., Rorden, C., Pambakian, A., Kennard, C., et al. (2003). The anatomy of visual neglect. *Brain, 126,* 1986–1997.
Naccache, L., Slachevsky, A., Levy, R., & Dubois, B. (2000). Simultanagnosia in a patient with right brain lesions. *Journal of Neurology, 247,* 650–651.
Ogren, M. P., Mateer, C. A., & Wyler, A. R. (1984). Alterations in visually related eye movements following left pulvinar damage in man. *Neuropsychologia, 22,* 187–196.
Ota, H., Fujii, T., Suzuki, K., Fukatsu, R., & Yamadori, A. (2001). Dissociation of body-centered and stimulus-centered representations in unilateral neglect. *Neurology, 57,* 2064–2069.
Petrides, M., & Pandya, D. N. (2006). Efferent association pathways originating in the caudal prefrontal cortex in the macaque monkey. *Journal of Comparative Neurology, 498,* 227–251.
Riddoch, M. J., Chechlacz, M., Mevorach, C., Mavritsaki, E., Allen, H., & Humphreys, G. W. (2010). The neural mechanisms of visual selection: The view from neuropsychology. *Annals of the New York Academy of Sciences, 1191,* 156–181.
Rizzo, M., & Hurtig, R. (1987). Looking but not seeing: Attention, perception, and eye movements in simultanagnosia. *Neurology, 37,* 1642–1648.
Rizzo, M., & Vecera, S. P. (2002). Psychoanatomical substrates of Balint's syndrome. *Journal of Neurology, Neurosurgery and Psychiatry, 72,* 162–178.
Robertson, I. H., & Manly, T. (1999). Sustained attention deficits in time and space. In G. W. Humphreys, J. A. Duncan, & A. Treisman (Eds.), *Attention, space and action: Studies in cognitive neuroscience* (pp. 297–310). Oxford, UK: Oxford University Press.
Robertson, L., Treisman, A., Friedman-Hill, S., & Grabowecky, M. (1997). The interaction of spatial and object pathways: Evidence from Balint's syndrome. *Journal of Cognitive Neuroscience, 9,* 295–317.
Schmahmann, J. D., & Pandya, D. N. (2006). *Fiber pathways of the brain*. New York: Oxford University Press.

Seghier, M. L., Ramlackhansingh, A., Crinion, J., Leff, A. P., & Price, C. J. (2008). Lesion identification using unified segmentation-normalisation models and fuzzy clustering. *Neuroimage, 41,* 1253–1266.
Shalev, L., Humphreys, G. W., & Mevorach, C. (2005). Global processing of compound letters in a patient with Balint's syndrome. *Cognitive Neuropsychology, 22,* 737–751.
Shalev, L., Mevorach, C., & Humphreys, G. W. (2007). Local capture in Balint's syndrome: Effects of grouping and item familiarity. *Cognitive Neuropsychology, 24,* 115–127.
Singh, M., Jeong, J., Hwang, D., Sungkarat, W., & Gruen, P. (2010). Novel diffusion tensor imaging methodology to detect and quantify injured regions and affected brain pathways in traumatic brain injury. *Magnetic Resonance Imaging, 28,* 22–40.
Smith, S. M., Jenkinson, M., Woolrich, M. W., Beckmann, C. F., Behrens, T. E., Johansen-Berg, H., et al. (2004). Advances in functional and structural MR image analysis and implementation as FSL. *Neuroimage, 23(Suppl. 1),* S208–S219.
Stamatakis, E. A., & Tyler, L. K. (2005). Identifying lesions on structural brain images—Validation of the method and application to neuropsychological patients. *Brain and Language, 94,* 167–177.
Stasheff, S. F., & Barton, J. J. (2001). Deficits in cortical visual function. *Ophthalmology Clinics of North America, 14,* 217–242, x.
Thiebaut de Schotten, M., Kinkingnehun, S., Delmaire, C., Lehericy, S., Duffau, H., Thivard, L., et al. (2008). Visualization of disconnection syndromes in humans. *Cortex, 44,* 1097–1103.
Thomas, C., Avidan, G., Humphreys, K., Jung, K. J., Gao, F., & Behrmann, M. (2009). Reduced structural connectivity in ventral visual cortex in congenital prosopagnosia. *Nature Neuroscience, 12,* 29–31.
Thomas, C., Moya, L., Avidan, G., Humphreys, K., Jung, K. J., Peterson, M. A., et al. (2008). Reduction in white matter connectivity, revealed by diffusion tensor imaging, may account for age-related changes in face perception. *Journal of Cognitive Neuroscience, 20,* 268–284.
Tusa, R. J., & Ungerleider, L. G. (1985). The inferior longitudinal fasciculus: A reexamination in humans and monkeys. *Annals of Neurology, 18,* 583–591.
Tzourio-Mazoyer, N., Landeau, B., Papathanassiou, D., Crivello, F., Etard, O., Delcroix, N., et al. (2002). Automated anatomical labeling of activations in SPM using a macroscopic anatomical parcellation of the MNI MRI single-subject brain. *Neuroimage, 15,* 273–289.
Umarova, R. M., Saur, D., Schnell, S., Kaller, C. P., Vry, M. S., Glauche, V., et al. (2010). Structural connectivity for visuospatial attention: Significance of ventral pathways. *Cerebral Cortex, 20,* 121–129.
Urbanski, M., Thiebaut de Schotten, M., Rodrigo, S., Catani, M., Oppenheim, C., Touze, E., et al. (2008). Brain networks of spatial awareness: Evidence from diffusion tensor imaging tractography. *Journal of Neurology, Neurosurgery and Psychiatry, 79,* 598–601.
Vallar, G. (2001). Extrapersonal visual unilateral spatial neglect and its neuroanatomy. *Neuroimage, 14,* S52–S58.
Vallar, G., Bottini, G., & Paulesu, E. (2003). Neglect syndromes: The role of the parietal cortex. *Advances in Neurology, 93,* 293–319.
Verdon, V., Schwartz, S., Lovblad, K. O., Hauert, C. A., & Vuilleumier, P. (2010). Neuroanatomy of hemispatial neglect and its functional components: A study using voxel-based lesion-symptom mapping. *Brain, 133,* 880–894.
Wolpert, I. (1924). Die Simultanagnosie. Zeitschrift für die gesamte. *Neurologie und Psychiatry, 93,* 397–415.
Woolsey, T. A., Hanaway, J., & Gado, M. H. (2008). *The brain atlas: A visual guide to the human central nervous system* (3rd ed.). Hoboken, NJ: Wiley.
Worsley, K. J. (2003). Developments in random field theory. In R. S. J. Frackowiak et al. (Eds.), *Human brain function* (2nd ed., pp. 881–886). San Diego, CA: Academic Press.